

Beauty Hadron Spectrum in a Screened Potential Model

Raghavendra Kaushal* and Bhaghyesh†

Department of Physics, Manipal Institute of Technology,
Manipal Academy of Higher Education, Manipal, Karnataka, India, 576104

The mass spectrum of beauty hadrons ($b\bar{b}$ and bbb baryons) and bb -diquarks are computed in a non-relativistic phenomenological potential model. The potential comprises of a short-range Coulomb potential, a screened confinement potential, and $O(1/m)$ corrections predicted from lattice and pNRQCD studies. Among the spin-dependent interactions, spin-spin interaction is considered non-perturbatively, whereas spin-orbit and tensor interactions are considered perturbatively. The Matrix-Numerov method is used to numerically solve the non-relativistic Schrodinger equation to evaluate the mass spectra. We interpret $\Upsilon(10753)$ as D -wave bottomonium state and $\Upsilon(10860)$ and $\Upsilon(11020)$ as S -wave bottomonium states. The mass spectrum of bbb baryons are evaluated under the diquark-quark model. The excited masses are computed by considering various radial and orbital excitations of the diquark as well as the diquark-quark system.

Keywords: Bottomonium, Screened confinement potential, Diquark-quark model, Triply bottom baryons, $O(1/m)$ corrections, Matrix-Numerov method.

I. INTRODUCTION

The study of beauty hadrons (B-hadrons) is an interesting area of research as it allows one to explore the interplay between perturbative and non-perturbative quantum chromodynamics [1, 2]. It also plays a crucial role in determining the matrix elements of the CKM (Cabibbo-Kobayashi-Maskawa) matrix [3, 4]. The discovery of $\Upsilon(1S)$, a bottomonium state ($b\bar{b}$) in the year 1977 marked the beginning of a new field called B-physics. $\Upsilon(1S)$ was observed by E288 Collaboration (Fermilab) while analyzing the spectrum of dimuons ($\mu^+\mu^-$) produced by the collision of a protons with Pb and Cu targets at 400 GeV [5, 6]. The orbitally excited bottomonium states $\chi_{bJ}(1P)$ were confirmed by analyzing the electromagnetic spectrum of $\Upsilon(2S)$ obtained at DESY [7]. CLEO collaboration [8] presented the first evidence for the existence of D-wave bottomonium state $\Upsilon(1D)$ by analyzing the decays, $\Upsilon(3S) \rightarrow \gamma\chi_b(2P_J)$, $\chi_b(2P_J) \rightarrow \gamma\Upsilon(1D)$. In the last three decades, the bottomonium sector has evolved exceptionally due to the extraordinary efforts by various collaborations like CLEO collaboration [8–11], Belle collaboration [12–14], BaBar collaboration [15–18], ATLAS collaboration [19], CMS collaboration [20], and LHCb collaboration [21] to name few. In 2007, the CDF collaboration [22] reported the first observation of beauty baryons produced at the Tevatron from the proton-antiproton collisions at 1.1 fb^{-1} . They interpreted the discovered states as Σ_b^+ with mass $5807.8_{-2.2}^{+2.0} \pm 1.7 \text{ MeV}/c^2$ and Σ_b^- with mass $5815.2 \pm 1.0 \pm 1.7 \text{ MeV}/c^2$. Currently, we have several baryons that consist of a single bottom quark ($\Lambda_b^0, \Sigma_b^0, \Sigma_b^+, \Sigma_b^-, \Xi_b^0, \Xi_b^-,$ and Ω_b^-), but baryons consisting of two or three bottom quarks have not been discovered yet [23]. The authors of Ref. [24] computed the fragmentation functions for triply charmed (Ω_{ccc}) and triply bottom (Ω_{bbb}) baryons by applying the perturbation theory in Feynman gauge by incorporating contributions from two Feynman diagrams. They obtained the fragmentation probability for Ω_{ccc} and Ω_{bbb} of the order of 10^{-9} , which they believe can be observed at LHC because of its high collision rates. However, the authors of Ref. [25] argue that this computed fragmentation function is not accurately described as there will be a minimum of seven Feynman diagrams that would contribute to the fragmentation function. Nevertheless, their calculations show that at an integrated luminosity of 10 fb^{-1} at LHC, there could be 10^4 to 10^5 events of triply heavy baryons and concluded that it is quite favorable for triply heavy baryons to be discovered at LHC. Investigating bottom-quark physics is essential as it allows us to examine the flavor dynamics of the Standard Model and may uncover the reasons behind the existence of three generations of particles in nature. The study of B-hadrons are regarded as an important pathway for grasping the fundamental principles of particle physics [26]. Due to the higher mass of bottom quarks compared to charm or other light quarks, the behavior of bottom quarks in the quark-gluon plasma changes from losing energy to diffusion. Examining beauty hadrons can offer crucial information about the shift from high-energy parton movement to low-energy diffusion, which plays a key role in comprehending the dynamics of the quark-gluon plasma [27].

Various theoretical approaches such as effective field theories [28–31], lattice QCD [32–34], and phenomenological potential models [35–38] are used to study the spectra of beauty hadrons. The theoretical study of triply bottom baryons is anticipated to provide essential insights for future experimental endeavors. Various theoretical approaches employed to investigate the spectra of triply bottom baryons include the constituent quark model [39–42], QCD

* Raghavendra Kaushal: kaushalraghavendra23@gmail.com

† Bhaghyesh (Corresponding author): bhaghyesh.mit@manipal.edu

sum rules [43–45], diquark-quark model [35, 46], lattice QCD [34, 47], and the hypercentral constituent quark model [48, 49]. The existing literature suggests that there has been insufficient investigation into the excited states of triply bottom baryons. The quark models effectively describe various properties of baryons, such as mass spectra, magnetic moments, form factors, strong decays, and so on. Nonetheless, these models predict a greater number of states than what has been observed in experiments (for lighter baryons). This discrepancy is known as the missing resonance problem [50, 51]. An alternative solution to this problem is to use models that utilize less number of effective degrees of freedom compared to the traditional three-quark model for baryons. This has led to the development of the quark-diquark model for baryons [52]. In this work, we employ the diquark-quark approach to investigate the mass spectrum of triply bottom baryons. Diquark, as the name suggests, is a (hypothetical) bound state of two quarks [52–54]. Diquarks are colored and hence cannot be found as an isolated particle. The significance of modelling baryons as a bound state of diquark and quark is that the color interaction between diquark and quark is similar to that of an antiquark and quark in mesons [55]. In this work, we compute the mass spectra of bottomonium, bb -diquarks, and triply bottom baryons utilizing a non-relativistic phenomenological potential model with one-gluon Coulomb-like short-range potential and the screened confinement potential. In the literature, we observed that most of the phenomenological potential models use linear confinement potential. It is because the linear confinement potential can be obtained from Yang-Mills gauge theories and also certain lattice results support this [56, 57]. There are various other confinement potentials used in the literature (for detailed review refer [58]). We will be utilizing the screened confinement potential, as it has been found that with the increasing separation between the quarks, dynamic quark-antiquark pairs may emerge from the vacuum, leading to vacuum polarization. As a result of this, the interquark potential will be subject to screening [56, 59]. Furthermore, we incorporate the $O(1/m)$ corrections derived from LQCD [60] and pNRQCD [28], which are simulated using the quenched approximation. These corrections are attributed to the nonzero masses of the heavy quarks. Our work integrates quenched $O(1/m)$ corrections with a screened confinement potential, establishing a link between the theoretical frameworks influenced by quenched QCD and practical representations that take into account the unquenched effects.

The paper is structured as follows. In section II, we have given the theoretical framework where we have discussed the potential model and the method employed to numerically solve the Schrodinger wave equation to evaluate the mass spectra of beauty hadrons ($b\bar{b}$ and bbb baryon). In section III, we have presented the mass spectra of beauty hadrons and have compared with other theoretical approaches and available experimental results. In section IV, we have provided our conclusions.

II. THEORETICAL FRAMEWORK:

In systems consisting of heavy quarks, the kinetic energy of the individual quarks is negligible compared to their rest mass energy. Hence it is favorable to model these systems using a non-relativistic approach. To evaluate the mass spectra, we make use of nonrelativistic radial Schrodinger equation given by,

$$\left[\frac{1}{2\mu} \left(-\frac{d^2}{dr^2} + \frac{l(l+1)}{r^2} \right) + V(r) \right] u(r) = Eu(r). \quad (1)$$

Here μ corresponds to the reduced mass of the system, $\mu = (m_1 m_2)/(m_1 + m_2)$, l to the relative orbital angular momentum of the system, and r to the interquark separation respectively. Equation (1) will be solved numerically. In the literature, we can find various numerical methods to solve the Schrodinger equation. Prominent among them are Discrete Variable Representation (DVR) method [61], Nikiforov-Uvarov (NU) method [62], Runge-Kutta Method [63], Matrix Numerov Method [64], Fourier grid Hamiltonian method [65], Variational method [66], Phase Integral method [67], and Asymptotic Iteration method [68]. In this work, we use the Matrix Numerov method because of its efficiency in simultaneously computing multiple eigenstates [64]. The method is briefly outlined as follows:

Equation (1) is rewritten as,

$$\frac{d^2 u(r)}{dr^2} = - \left(2\mu E - V(r) - \frac{l(l+1)}{r^2} \right) u(r) = g(r)u(r). \quad (2)$$

with $g(r) = - \left(2\mu E - V(r) - \frac{l(l+1)}{r^2} \right)$. The space will be discretized into N equal parts that are separated by a distance d . The second derivative of $u(r)$ in equation (2) will be approximated using Taylor series expansion of $u(r)$.

$$u(r \pm d) = u(r) \pm du^{(1)}(r) + \frac{1}{2!} d^2 u^{(2)}(r) \pm \frac{1}{3!} d^3 u^{(3)}(r) + \frac{1}{4!} d^4 u^{(4)}(r) + \dots \quad (3)$$

with $u^{(n)}(r) = \frac{d^n u(r)}{dr^n}$. From equation (3), the second derivative of $u(r)$ can be written as,

$$u^{(2)}(r) = \frac{u(r+d) + u(r-d) - 2u(r)}{d^2} - \frac{1}{12} d^2 u^{(4)}(r) + O(d^4) \quad (4)$$

Substituting equation (4) in equation (2) and rearranging, we get,

$$u^{(4)}(r) = \frac{g(r+d)u(r+d) + g(r-d)u(r-d) - 2g(r)u(r)}{d^2} + O(d^2) \quad (5)$$

Substituting equation (5) in equation (4) and rearranging, we get,

$$g_j u_j = \frac{u_{j+1} + u_{j-1} - 2u_j}{d^2} - \frac{1}{12} (g_{j+1}u_{j+1} + g_{j-1}u_{j-1} - 2g_j u_j) \quad (6)$$

Here $g_{j-1} = g(r-d)$, $g_j = g(r)$, $g_{j+1} = g(r+d)$, $u_{j-1} = u(r-d)$, $u_j = u(r)$, $u_{j+1} = u(r+d)$. By comparing equations (6) and (2), the Schrodinger equation in matrix form can be written as [64, 69],

$$\left[-\frac{1}{2\mu}(AB^{-1}) + \frac{l(l+1)}{2\mu r_j^2} + V(r_j) \right] u_j = E u_j. \quad (7)$$

with $u_j = u(r_j)$ is the wavefunction at r_j , $r_j = r_{min} + jd$, $d = (r_{max} - r_{min})/N$, r_{max} and r_{min} are the upper and lower bounds of the space under consideration, d is the distance between the two discretized points, $A = (I_{-1} - 2I_0 + I_1)/d^2$, $B = (I_{-1} + 10I_0 + I_1)/12$, I_{-1} , I_0 , and I_1 are lower, diagonal unit matrix, and upper shift matrix respectively i.e.

$$I_{-1} = \begin{pmatrix} 0 & 0 & \cdots \\ 1 & 0 & \cdots \\ \vdots & 1 & \ddots \end{pmatrix}, I_0 = \begin{pmatrix} 1 & 0 & 0 & \cdots \\ 0 & 1 & 0 & \cdots \\ \vdots & 0 & 0 & \ddots \end{pmatrix}, I_1 = \begin{pmatrix} 0 & 1 & 0 & \cdots \\ 0 & 0 & 1 & \cdots \\ \vdots & 0 & 0 & \ddots \end{pmatrix} \quad (8)$$

Equation (7) is solved using Wolfram Mathematica software. In this work, we take $N = 500$ and $r_{max} = 5$ fm.

Typically, the potentials in phenomenological potential models consists of both spin-independent and spin-dependent parts. Spin-dependent interaction comprises of spin-spin, spin-orbit, and tensor interactions. In the literature, we can observe that in most of the models, the spin-dependent interactions have been considered perturbatively. Nevertheless, it has been suggested in Refs [70, 71] that the spin-spin interaction plays an important role in the binding energy, making it more favorable to treat it in a non-perturbative manner. Therefore, we will be considering the spin-spin interaction non-perturbatively whereas spin-orbit and tensor interactions will be considered perturbatively. Spin-independent interaction usually comprises of one-gluon short-range Coulomb-like potential and the confinement potential. The potential that we will be employing to solve Schrodinger equation (7) includes one-gluon short-range Coulomb-like potential, screened confinement potential, $O(1/m)$ corrections, and the spin-spin interaction given by,

$$V(r) = \frac{\kappa\alpha_s(Q^2)}{r} + \frac{\lambda(1 - e^{-\nu r})}{\nu} + \left(\frac{1}{m_1} + \frac{1}{m_2} \right) \left(\frac{-9\alpha^2}{8r^2} + C \ln(ar) \right) + V_{SS}(r). \quad (9)$$

Here κ corresponds to color factor, λ is the string strength, ν is the screening factor, $\alpha_s(Q^2)$ is the QCD coupling constant at the renormalization scale Q , α is the effective coupling constant given by $\alpha = \kappa\alpha_s(Q^2)$, a and C are phenomenological constants, r is the interquark distance, m_1 and m_2 are the masses of constituent particles, and $V_{SS}(r)$ is the spin-spin interaction respectively. $\alpha_s(Q^2)$ is obtained by using the formula [72],

$$\alpha_s(Q^2) = \frac{4\pi}{\left(11 - \frac{2}{3}n_f\right) \ln\left(\frac{Q^2}{\Lambda_{QCD}^2}\right)}. \quad (10)$$

where Λ_{QCD} is the QCD scale whose value is around 0.1 to 0.4 GeV [23]. In this work, we have used $n_f = 4$ and $\Lambda_{QCD} = 0.130$ GeV. In the case of bottomonium, the renormalization scale Q will be equal to the mass of bottom quark (m_b). We will be using this same renormalization scale ($Q = m_b$) for bb diquark and triply bottom baryons.

The potential parameters are determined by considering the masses of 8 experimentally well-established bottomonium states ($\eta_b(1S)$, $\Upsilon(1S)$, $\eta_b(2S)$, $\Upsilon(2S)$, $\chi_{b0}(1P)$, $\chi_{b1}(1P)$, $h_b(1P)$, and $\chi_{b2}(1P)$) and by minimizing the chi-square, $\chi^2 = \sum_{i=1}^n ((M_i^{exp} - M_i^{cal})/\Delta M_i^{exp})^2$, where M_i^{exp} and M_i^{cal} are the experimental and calculated masses of the i^{th} bottomonium state respectively and ΔM_i^{exp} is the experimental uncertainty in the mass of i^{th} bottomonium state. We have taken a constant value for the experimental uncertainty, $\Delta M_i^{exp} = 5$ MeV as suggested in Ref [73]. This decision has been made due to the small and inconsistent experimental uncertainties in the masses of the states used for fitting. If the experimental uncertainty is excessively low, it will result in an overly precise mass, which can be unfavorable for fitting purposes [73]. The fitted potential parameters are shown in Table I.

TABLE I: Model Parameters.

m_b [GeV]	λ [GeV ²]	ν [GeV]	C [GeV]	a [GeV]	σ [GeV]
4.680	0.241	0.078	0.100	0.430	3.920

II.1. Bottomonium:

The color factor in equation (9) for bottomonium, which is a bound state of bottom and anti-bottom quarks will be $\kappa = -\frac{4}{3}$. Hence, the potential (9) for bottomonium takes the form,

$$V(r) = -\frac{4}{3} \frac{\alpha_s(m_b^2)}{r} + \frac{\lambda(1 - e^{-\nu r})}{\nu} + \left(\frac{1}{m_b} + \frac{1}{m_b} \right) \left(\frac{-9\alpha^2}{8r^2} + C \ln(ar) \right) + \frac{32\pi\alpha_s(m_b^2)}{9m_b^2} \left(\frac{\sigma}{\sqrt{\pi}} \right)^3 \exp(-\sigma^2 r^2) \mathbf{S}_1 \cdot \mathbf{S}_2. \quad (11)$$

In equation (11), the fourth term corresponds to smeared spin-spin interaction. Additionally, the other spin-dependent interactions such as spin-orbit and tensor interactions are given respectively as [74],

$$V_{LS}(r) = \frac{1}{2m_b^2 r} \left(3 \frac{dV_V(r)}{dr} - \frac{dV_S(r)}{dr} \right) \mathbf{L} \cdot \mathbf{S}. \quad (12)$$

$$V_T(r) = \frac{1}{12m_b^2} \left(\frac{1}{r} \frac{dV_V(r)}{dr} - \frac{d^2 V_V(r)}{dr^2} \right) S_{12}. \quad (13)$$

where,

$$S_{12} = 12 \left((\mathbf{S}_1 \cdot \hat{r})(\mathbf{S}_2 \cdot \hat{r}) - \frac{1}{3} \mathbf{S}_1 \cdot \mathbf{S}_2 \right). \quad (14)$$

Here $V_V(r)$ is a lorentz vector that corresponds to short-range interquark potential and $V_S(r)$ is a lorentz scalar that corresponds to the confinement potential. In this work, we take,

$$V_V(r) = \frac{\kappa\alpha_s}{r}, \quad V_S(r) = \frac{\lambda(1 - e^{-\nu r})}{r} \quad (15)$$

The masses of bottomonium states will be computed as,

$$M(b\bar{b}) = E + \langle V_{LS}(r) \rangle + \langle V_T(r) \rangle + 2m_b. \quad (16)$$

where E corresponds to the eigenvalue (binding energy) obtained by solving the Schrodinger equation (7), $\langle V_{LS}(r) \rangle$ and $\langle V_T(r) \rangle$ corresponds to perturbatively determined spin-orbit and tensor interaction energies respectively, and m_b corresponds to mass of bottom (antibottom) quark. The expectation values in equation (16) are evaluated using the wavefunctions obtained by solving the Schrodinger equation (7) for the potential given by equation (11).

II.2. $b\bar{b}$ diquarks:

In the fundamental color representation, quarks are represented by a color triplet $\mathbf{3}$ state [75]. The two quarks combine each other as $\mathbf{3} \otimes \mathbf{3} = \bar{\mathbf{3}} \oplus \mathbf{6}$. Here $\bar{\mathbf{3}}$ represents a color antitriplet state and $\mathbf{6}$ represents a color sextet state. The diquarks can either be in a color antitriplet state or in a color sextet state. Lets assume that the diquark is in color sextet state. The diquark combines with a quark as $\mathbf{6} \otimes \mathbf{3} = \mathbf{10} \oplus \mathbf{8}$. Here $\mathbf{10}$ represents a color decuplet state and $\mathbf{8}$ represents a color octet state. Since baryons are physically observable, it must be a color singlet ($\mathbf{1}$) state. Hence, diquarks cannot be in a color sextet state as the combination with quark does not give a color singlet state. Now, lets assume that the diquark is in color antitriplet state. The diquark combines with a quark as $\bar{\mathbf{3}} \otimes \mathbf{3} = \mathbf{1} \oplus \mathbf{8}$. This combination does give a color singlet state. Hence, the diquark will be in the color antitriplet state. In the fundamental color representation, antiquark is represented by an antitriplet state [75]. Therefore, this combination of antitriplet diquark with a quark in a baryon is identical to the combination of antitriplet antiquark with a quark

in a meson. Hence, the color interaction between diquark and quark in baryon is identical to the color interaction between antiquark and quark in meson [55] which is well studied and well understood.

As bb diquarks are made up of identical b quarks, according to Pauli Exclusion principle, the total wavefunction of the diquark system must be antisymmetric [52]. Parity of the diquark, given by $(-1)^{l_d}$ describes the nature of the spatial wavefunction, where l_d is the relative orbital angular momentum of the diquark. Since the flavor of quarks under consideration are same, the flavor wavefunction is symmetric. For color antitriplet diquark state, the color wavefunction is antisymmetric [55]. This suggests that for bb diquark, the color-flavor wavefunction is antisymmetric. Therefore, in order to have total wavefunction antisymmetric, the spin-spatial wavefunction must be symmetric.

For the diquark in the antitriplet color state, the color factor between the interaction of two quarks will be $\kappa = -\frac{2}{3}$ which is half the color factor between the interaction of a quark and an antiquark. It has been suggested in Refs [70, 76] that this factor of $\frac{1}{2}$ arises because of the color wavefunction and that it has to be considered for the entire static potential. Hence, we have the static potential for diquark as,

$$V_{qq}^{(0)}(r) = \frac{V_{q\bar{q}}^{(0)}(r)}{2} = -\frac{2}{3} \frac{\alpha_s(m_b^2)}{r} + \frac{\lambda(1 - e^{-\nu r})}{2\nu} \quad (17)$$

Including the $O(1/m)$ corrections and the spin-spin interactions, we get the diquark potential as,

$$V_{qq}(r) = -\frac{2}{3} \frac{\alpha_s(m_b^2)}{r} + \frac{\lambda(1 - e^{-\nu r})}{2\nu} + \left(\frac{1}{m_b} + \frac{1}{m_b} \right) \left(\frac{-9\alpha^2}{8r^2} + C \ln(ar) \right) + \frac{16\pi\alpha_s(m_b^2)}{9m_b^2} \left(\frac{\sigma}{\sqrt{\pi}} \right)^3 \exp(-\sigma^2 r^2) \mathbf{S}_1 \cdot \mathbf{S}_2. \quad (18)$$

The contributions from spin-orbit and tensor interactions will be computed perturbatively, using the formula given by equations (12) and (13).

II.3. Triply bottom baryons:

The mass spectrum of the triply bottom baryons are evaluated within the quark-diquark approach. The baryon is treated as a bound state of a bb -diquark and a b -quark, pictorially represented in Figure 1. We consider the same model parameters as given in Table I for the evaluation of mass spectrum of triply bottom baryons. In this work, the baryon states will be represented as ' $n_d l_d n L$ ' where n_d and l_d represents the radial and orbital quantum numbers of the diquark system respectively and n and L represents the radial and orbital quantum numbers of diquark-quark system respectively. The total wavefunction of baryon is a combination of spin, flavor, spatial, and color wavefunctions given by,

$$\psi_{baryon} = \psi_{spin} \psi_{flavor} \psi_{spatial} \psi_{color} \quad (19)$$

The total wavefunction must be antisymmetric in accordance with Pauli Exclusion principle [35]. For bbb baryon, the flavor wavefunction will be symmetric, color wavefunction will be antisymmetric, requiring the spin-spatial wavefunction to be symmetric. The spatial wavefunction depends on the parity of the baryon given by $(-1)^{l_d+L}$ where l_d is the relative orbital angular momentum of diquark and L is the relative orbital angular momentum of diquark-quark system respectively.

The spin-dependent interactions for baryons under the diquark-quark approach are similar to spin-dependent interactions in heavy open-flavored mesons. The spin-dependent interactions are given by [77–79],

$$V_{SS}(r) = \frac{32\pi\alpha_s}{9m_d m_q} \left(\frac{\sigma}{\sqrt{\pi}} \right)^3 \exp(-\sigma^2 r^2) \mathbf{J}_d \cdot \mathbf{S}_q. \quad (20)$$

$$V_{LS}(r) = \frac{4}{3} \alpha_s \frac{1}{m_d m_q r^3} \mathbf{L} \cdot \mathbf{S} + \left(\frac{1}{2m_d^2} \mathbf{L} \cdot \mathbf{J}_d + \frac{1}{2m_q^2} \mathbf{L} \cdot \mathbf{S}_q \right) \frac{1}{r} \frac{d}{dr} (V_V(r) - V_S(r)). \quad (21)$$

$$V_T(r) = \frac{-4\alpha_s [(\mathbf{L} \cdot \mathbf{J}_d)(\mathbf{L} \cdot \mathbf{S}_q) + (\mathbf{L} \cdot \mathbf{S}_q)(\mathbf{L} \cdot \mathbf{J}_d) - \frac{2}{3} L(L+1)(\mathbf{J}_d \cdot \mathbf{S}_q)]}{m_d m_q r^3 (2L-1)(2L+3)}. \quad (22)$$

Here m_q and m_d corresponds to the masses of constituent quark and diquark respectively, \mathbf{J}_d corresponds to total angular momentum of diquark given by, $\mathbf{J}_d = \mathbf{l}_d + \mathbf{S}_d$, \mathbf{S}_d and \mathbf{l}_d corresponds to total spin and relative orbital angular

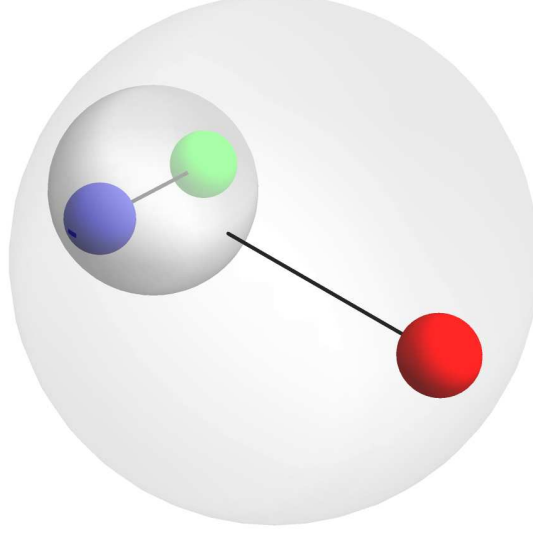


FIG. 1: Pictorial representation of baryon in diquark-quark model.

momentum of diquark respectively, \mathbf{L} corresponds to relative orbital angular momentum of diquark-quark system, and \mathbf{S}_q corresponds to spin of the quark interacting with diquark. In diquark-quark model, \mathbf{J}_d will be considered as the spin of diquark [36]. \mathbf{S} corresponds to the total spin of baryon given by, $\mathbf{S} = \mathbf{S}_q + \mathbf{J}_d$. Application of Pauli Exclusion principle for diquarks results in S -wave diquark with $\mathbf{J}_d = 1$, P -wave diquark with $\mathbf{J}_d = 1$, and D -wave diquark with $\mathbf{J}_d = 1, 2, 3$. The mass difference across different \mathbf{J}_d values for D -wave diquarks were found to be negligible (refer Table VII). Hence, for the computation of baryon masses, we consider S , P , and D -wave diquark with $\mathbf{J}_d = 1$ (if we were to consider D -wave diquark with $\mathbf{J}_d = 2, 3$, there could be mixing between states). The spin-orbit and tensor interactions will be evaluated in $|J; S\rangle$ basis. The basis transformation relation between $|J; j_q\rangle$ and $|J; S\rangle$ basis is given by [36],

$$|J; j_q\rangle = \sum_S (-1)^{J+L+J_d+S_q} \sqrt{(2S+1)(2j_q+1)} \begin{Bmatrix} J_d & S_q & S \\ L & J & j_q \end{Bmatrix} |J; S\rangle. \quad (23)$$

In $|J; j_q\rangle$ basis, the coupling takes place as follows. First, the relative orbital angular momentum of diquark-quark system \mathbf{L} couples with the spin of the quark \mathbf{S}_q to form \mathbf{j}_q i.e., $\mathbf{L} + \mathbf{S}_q = \mathbf{j}_q$. Then, \mathbf{j}_q couples with the total spin of diquark \mathbf{J}_d to form the total angular momentum \mathbf{J} of baryon i.e., $\mathbf{j}_q + \mathbf{J}_d = \mathbf{J}$. In $|J; S\rangle$ basis, coupling takes place as follows. First, the total spin of diquark \mathbf{J}_d couples with the spin of quark \mathbf{S}_q to form the total spin of baryon \mathbf{S} i.e., $\mathbf{J}_d + \mathbf{S}_q = \mathbf{S}$. Then, the total spin of baryon couples with the relative orbital angular momentum of diquark-quark system \mathbf{L} to form the total angular momentum \mathbf{J} of baryon i.e., $\mathbf{S} + \mathbf{L} = \mathbf{J}$. In equation (23), $|J; j_q\rangle$ basis is represented in terms of $|J; S\rangle$ basis. However, we will be using $|J; S\rangle$ basis represented in terms of $|J; j_q\rangle$ basis. We have given the basis states that are used in the evaluation of spin-orbit and tensor interactions in Table II.

III. RESULTS AND DISCUSSIONS:

III.1. Bottomonium:

We have evaluated the mass spectra of S , P , and D -wave bottomonium states and have compared our results with available experimental and other theoretical models in Tables III, IV, and V respectively. Graphical comparison of our results with PDG data [23] are presented in Figure 2. The $1S$, $2S$, $1P$, and $2P$ states are experimentally well established states and we can observe from Tables III, IV, and Figure 2 that the masses predicted from our model for these states align close to the experimental values. The experimental mass difference between $\Upsilon(1S)$ and $\eta_b(1S)$ is 62.3 ± 3.2 MeV [23] and we obtain this difference as 57 MeV. The Babar collaboration [18] reported the mass

TABLE II: $|J; S\rangle$ wavefunctions in terms of $|J; j_q\rangle$.

States	L	S	J	j_q	$ J; S\rangle$	$ J; j_q\rangle$
$1S1p, 2S1p, 1S2p, 2S2p$	1	$\frac{1}{2}$	$\frac{1}{2}$	$\frac{1}{2}, \frac{3}{2}$	$ \frac{1}{2}, \frac{1}{2}\rangle$	$-\frac{1}{3} \frac{1}{2}, \frac{1}{2}\rangle + \frac{2\sqrt{2}}{3} \frac{1}{2}, \frac{3}{2}\rangle$
	1	$\frac{1}{2}$	$\frac{3}{2}$	$\frac{1}{2}, \frac{3}{2}$	$ \frac{3}{2}, \frac{1}{2}\rangle$	$-\frac{2}{3} \frac{3}{2}, \frac{1}{2}\rangle + \frac{\sqrt{5}}{3} \frac{3}{2}, \frac{3}{2}\rangle$
$1S1d, 2S1d, 1S2d, 2S2d$	2	$\frac{3}{2}$	$\frac{3}{2}$	$\frac{3}{2}, \frac{5}{2}$	$ \frac{3}{2}, \frac{3}{2}\rangle$	$\frac{2}{\sqrt{5}} \frac{3}{2}, \frac{3}{2}\rangle + \frac{1}{\sqrt{5}} \frac{3}{2}, \frac{5}{2}\rangle$
	2	$\frac{3}{2}$	$\frac{5}{2}$	$\frac{3}{2}, \frac{5}{2}$	$ \frac{5}{2}, \frac{3}{2}\rangle$	$\sqrt{\frac{7}{15}} \frac{5}{2}, \frac{3}{2}\rangle + 2\sqrt{\frac{2}{15}} \frac{5}{2}, \frac{5}{2}\rangle$
$1P1p, 2P1p, 1P2p, 2P2p$	1	$\frac{3}{2}$	$\frac{1}{2}$	$\frac{1}{2}, \frac{3}{2}$	$ \frac{1}{2}, \frac{3}{2}\rangle$	$\frac{2\sqrt{2}}{3} \frac{1}{2}, \frac{1}{2}\rangle + \frac{1}{3} \frac{1}{2}, \frac{3}{2}\rangle$
	1	$\frac{3}{2}$	$\frac{3}{2}$	$\frac{1}{2}, \frac{3}{2}$	$ \frac{3}{2}, \frac{3}{2}\rangle$	$\frac{\sqrt{5}}{3} \frac{3}{2}, \frac{1}{2}\rangle + \frac{2}{3} \frac{3}{2}, \frac{3}{2}\rangle$
$1P1d, 2P1d, 1P2d, 2P2d$	2	$\frac{1}{2}$	$\frac{3}{2}$	$\frac{3}{2}, \frac{5}{2}$	$ \frac{3}{2}, \frac{1}{2}\rangle$	$-\frac{1}{\sqrt{5}} \frac{3}{2}, \frac{3}{2}\rangle + \frac{2}{\sqrt{5}} \frac{3}{2}, \frac{5}{2}\rangle$
	2	$\frac{1}{2}$	$\frac{5}{2}$	$\frac{3}{2}, \frac{5}{2}$	$ \frac{5}{2}, \frac{1}{2}\rangle$	$-2\sqrt{\frac{2}{15}} \frac{5}{2}, \frac{3}{2}\rangle + \sqrt{\frac{7}{15}} \frac{5}{2}, \frac{5}{2}\rangle$
$1D1p, 2D1p, 1D2p, 2D2p$	1	$\frac{1}{2}$	$\frac{1}{2}$	$\frac{1}{2}, \frac{3}{2}$	$ \frac{1}{2}, \frac{1}{2}\rangle$	$-\frac{1}{3} \frac{1}{2}, \frac{1}{2}\rangle + \frac{2\sqrt{2}}{3} \frac{1}{2}, \frac{3}{2}\rangle$
	1	$\frac{1}{2}$	$\frac{3}{2}$	$\frac{1}{2}, \frac{3}{2}$	$ \frac{3}{2}, \frac{1}{2}\rangle$	$-\frac{2}{3} \frac{3}{2}, \frac{1}{2}\rangle + \frac{\sqrt{5}}{3} \frac{3}{2}, \frac{3}{2}\rangle$
$1D1d, 2D1d, 1D2d, 2D2d$	2	$\frac{3}{2}$	$\frac{3}{2}$	$\frac{3}{2}, \frac{5}{2}$	$ \frac{3}{2}, \frac{3}{2}\rangle$	$\frac{2}{\sqrt{5}} \frac{3}{2}, \frac{3}{2}\rangle + \frac{1}{\sqrt{5}} \frac{3}{2}, \frac{5}{2}\rangle$
	2	$\frac{3}{2}$	$\frac{5}{2}$	$\frac{3}{2}, \frac{5}{2}$	$ \frac{5}{2}, \frac{3}{2}\rangle$	$\sqrt{\frac{7}{15}} \frac{5}{2}, \frac{3}{2}\rangle + 2\sqrt{\frac{2}{15}} \frac{5}{2}, \frac{5}{2}\rangle$

difference between $\chi_{b1}(1P)$ and $\chi_{b0}(1P)$ as 32.5 ± 0.9 MeV and from our model, we obtain this difference as 25 MeV. The reported mass difference between $\chi_{b2}(1P)$ and $\chi_{b1}(1P)$ by PDG [23] is 19.10 ± 0.25 MeV and we obtain this difference as 8 MeV. The mass difference between $\Upsilon(2S)$ and $\eta_b(2S)$ reported by Belle Collaboration [12] which also reported the first evidence of $\eta_b(2S)$ is $24.3 \pm 3.5^{+2.8}_{-1.9}$ MeV and from our model, we obtain this difference as 22 MeV, which is well within the experimental uncertainty. The reported mass difference between $\chi_{b1}(2P)$ and $\chi_{b0}(2P)$ by BaBar collaboration [17] is 23.8 ± 1.7 MeV and we obtain this difference as 13 MeV. The mass difference between $\chi_{b2}(2P)$ and $\chi_{b1}(2P)$ reported by PDG [23] is 13.10 ± 0.24 MeV and our model gives this difference as 7 MeV. Under $3S$ and $4S$ states, we only have spin triplet states discovered, $\Upsilon(3S)$ and $\Upsilon(4S)$ respectively with the experimental mass of 10355.1 ± 0.5 MeV and 10579.4 ± 1.2 MeV respectively [23]. The predicted masses for these states from our model are 10351 MeV and 10614 MeV respectively. The mass difference reported by BaBar collaboration [18] between $\Upsilon(3S)$ and $\Upsilon(2S)$ is $331.50 \pm 0.02 \pm 0.13$ MeV and from our model, this difference is 340 MeV. Under $3P$ states, we only have $\chi_{b1}(3P)$ and $\chi_{b2}(3P)$ with experimental masses of 10513.4 ± 0.7 MeV and 10524.0 ± 0.8 MeV respectively [23]. The predicted masses of these states from our model are 10540 MeV and 10547 MeV respectively. For D -wave bottomonium state, we only have 1 experimentally observed state $\Upsilon_2(1D)$ corresponding to $J^{PC} = 2^{--}$ which is a 1^3D_2 state. The experimental mass of $\Upsilon_2(1D)$ is 10163.7 ± 1.4 MeV [23]. The predicted mass for this state from our model is 10158 MeV.

We have assigned 3 experimentally observed states by comparing their J^{PC} values and their observed masses with those predicted from our model. $\Upsilon(10753)$ with observed mass of 10753 ± 6 MeV [23] is assigned as 3^3D_1 state with predicted mass of 10685 MeV. We have assigned $\Upsilon(10860)$ with observed mass of $10885.2^{+2.6}_{-1.6}$ MeV [23] as 5^3S_1 state with predicted mass of 10833 MeV. $\Upsilon(11020)$ with experimental mass of 11000 ± 4 MeV [23] is assigned as 6^3S_1 state with predicted mass of 11022 MeV. We can observe from Figure 2 that below $B\bar{B}$ threshold, the predicted masses from our model lies close to the experimental values, whereas above this threshold, there are slight deviations. Above $B\bar{B}$ threshold, there are at present 4 experimental states $\Upsilon(4S)$, $\Upsilon(10860)$, $\Upsilon(11020)$, and $\Upsilon(10753)$. All these states corresponds to $J^{PC} = 1^{--}$ with the radial quantum number $n \geq 3$. These deviations arises because of the fact that there can be mixing between $(n+1)S$ state and nD state ($S-D$ mixing) [83–85] which we have not considered in this work. This mixing becomes significant for $n \geq 3$ [83] and hence we can observe that only for $n \geq 3$, the deviations are large whereas for $n < 3$, the deviations are negligible for $J^{PC} = 1^{--}$. There can also be coupled channel effects [86] above $B\bar{B}$ threshold, that can be responsible for these observed deviations. It is found in Ref. [83] that the difference in mass between nD state and $(n+1)S$ state is small and that the mass difference decreases with increase in n . This can be found in Table VI, where we have tabulated the mass difference between nD state and $(n+1)S$ state corresponding to $J^{PC} = 1^{--}$ obtained from our model.

TABLE III: Mass Spectra of S -wave Bottomonium in MeV.

State	J^{PC}	Meson	PDG [23]	Our Work	[38]	[37]	[80]	[81]	[82]
1^1S_0	0^{-+}	$\eta_b(1S)$	9398.7 ± 2.0	9401	9389	9399	9423	9412	9547
2^1S_0	0^{-+}	$\eta_b(2S)$	9999 ± 4	9989	9987	9986	9983	9995	9977
3^1S_0	0^{-+}			10335	10330	10315	10342	10339	10232
4^1S_0	0^{-+}			10602	10595	10583	10638	10572	10436
5^1S_0	0^{-+}			10823	10817	10816	10901	10746	10607
6^1S_0	0^{-+}			11014	11011	11024	11140	11064	
1^3S_1	1^{--}	$\Upsilon(1S)$	9460.40 ± 0.10	9458	9460	9470	9463	9460	9551
2^3S_1	1^{--}	$\Upsilon(2S)$	10023.4 ± 0.5	10011	10016	10033	10001	10026	9978
3^3S_1	1^{--}	$\Upsilon(3S)$	10355.1 ± 0.5	10351	10351	10352	10354	10364	10232
4^3S_1	1^{--}	$\Upsilon(4S)$	10579.4 ± 1.2	10614	10611	10615	10650	10594	10437
5^3S_1	1^{--}	$\Upsilon(10860)$	$10885.2^{+2.6}_{-1.6}$	10833	10831	10845	10912	10766	10607
6^3S_1	1^{--}	$\Upsilon(11020)$	11000 ± 4	11022	11023	11051	11151	11081	

TABLE IV: Mass Spectra of P -wave Bottomonium in MeV.

State	J^{PC}	Meson	PDG [23]	Our Work	[38]	[37]	[80]	[81]	[82]
1^1P_1	1^{+-}	$h_b(1P)$	9899.3 ± 0.8	9914	9903	9864	9899	9874	9905
2^1P_1	1^{+-}	$h_b(2P)$	10259.8 ± 1.2	10268	10256	10298	10268	10270	10167
3^1P_1	1^{+-}			10542	10529	10555	10570	10526	10377
4^1P_1	1^{+-}			10769	10757	10785		10714	10556
5^1P_1	1^{+-}			10964	10955	10994		10863	
6^1P_1	1^{+-}			11136					
1^3P_0	0^{++}	$\chi_{b0}(1P)$	$9859.44 \pm 0.42 \pm 0.31$	9887	9865	9837	9874	9849	9892
2^3P_0	0^{++}	$\chi_{b0}(2P)$	$10232.5 \pm 0.4 \pm 0.5$	10253	10226	10258	10248	10252	10157
3^3P_0	0^{++}			10529	10502	10503	10551	10512	10368
4^3P_0	0^{++}			10757	10732	10727		10703	10549
5^3P_0	0^{++}			10953	10933	10930		10853	
6^3P_0	0^{++}			11126					
1^3P_1	1^{++}	$\chi_{b1}(1P)$	$9892.78 \pm 0.26 \pm 0.31$	9912	9897	9852	9894	9871	9904
2^3P_1	1^{++}	$\chi_{b1}(2P)$	$10255.46 \pm 0.22 \pm 0.50$	10266	10251	10279	10265	10267	10166
3^3P_1	1^{++}	$\chi_{b1}(3P)$	10513.4 ± 0.7	10540	10524	10529	10567	10524	10375
4^3P_1	1^{++}			10767	10753	10756		10713	10555
5^3P_1	1^{++}			10963	10951	10962		10861	
6^3P_1	1^{++}			11134					
1^3P_2	2^{++}	$\chi_{b2}(1P)$	$9912.21 \pm 0.26 \pm 0.31$	9920	9918	9877	9907	9881	9911
2^3P_2	2^{++}	$\chi_{b2}(2P)$	$10268.65 \pm 0.22 \pm 0.50$	10273	10269	10317	10274	10274	10171
3^3P_2	2^{++}	$\chi_{b2}(3P)$	10524.0 ± 0.8	10547	10540	10580	10576	10530	10380
4^3P_2	2^{++}			10774	10767	10814		10717	10559
5^3P_2	2^{++}			10969	10965	11026		10865	
6^3P_2	2^{++}			11140					

III.2. bb diquarks:

We have computed the mass spectra of S , P , and D -wave bb diquarks and have compared with other theoretical models and with the corresponding bottomonium states evaluated from our model in Table VII. In Figure 3, we have shown the comparison of the masses of bb -diquarks obtained from our model with other theoretical models. We can observe from Table VII that the masses of diquark obtained from our model is around 200 MeV less than those obtained from other models. For the excited states, the reason for this difference could be the use of different confinement potentials. However, in the case of lower states, it is evident that the Coulomb interaction dominates

TABLE V: Mass Spectra of D -wave Bottomonium in MeV.

State	J^{PC}	Meson	PDG [23]	Our Work	[38]	[37]	[80]	[81]	[82]
1^1D_2	2^{-+}			10157	10152	10140	10149	10153	10089
2^1D_2	2^{-+}			10448	10439	10519	10465	10456	10306
3^1D_2	2^{-+}			10687	10677	10733	10740	10664	10493
4^1D_2	2^{-+}			10892	10883	10940	10988	10823	10650
5^1D_2	2^{-+}			11071	11066	11145		10952	
6^1D_2	2^{-+}			11229				11057	
1^3D_1	1^{--}			10156	10145	10086	10145	10144	10086
2^3D_1	1^{--}			10446	10432	10451	10462	10450	10303
3^3D_1	1^{--}	$\Upsilon(10753)$	10753 ± 6	10685	10670	10652	10736	10659	10490
4^3D_1	1^{--}			10890	10877	10848	10985	10818	10648
5^3D_1	1^{--}			11069	11060	11047		10949	
6^3D_1	1^{--}			11228				11054	
1^3D_2	2^{--}	$\Upsilon_2(1D)$	10163.7 ± 1.4	10158	10151	10123	10149	10152	10089
2^3D_2	2^{--}			10448	10438	10497	10465	10455	10306
3^3D_2	2^{--}			10687	10676	10707	10740	10664	10493
4^3D_2	2^{--}			10892	10882	10909	10988	10822	10650
5^3D_2	2^{--}			11071	11065	11113		10951	
6^3D_2	2^{--}			11229				11057	
1^3D_3	3^{--}			10157	10156	10175	10150	10158	10091
2^3D_3	3^{--}			10449	10442	10563	10466	10459	10308
3^3D_3	3^{--}			10688	10680	10787	10741	10667	10495
4^3D_3	3^{--}			10893	10886	11000	10990	10825	10651
5^3D_3	3^{--}			11072	11069	11211		10954	
6^3D_3	3^{--}			11230				11059	

TABLE VI: Mass difference between nD state and $(n+1)S$ state in MeV corresponding to $J^{PC} = 1^{--}$

$nD - (n+1)S$	Mass Difference
$1D - 2S$	145
$2D - 3S$	95
$3D - 4S$	71
$4D - 5S$	57
$5D - 6S$	47

across all the models and hence the difference should be minimal. Nonetheless, in our model, we have incorporated $O(1/m)$ interactions which also significantly influence the lower states. This could be the reason for the discrepancy observed in the lower states. If we were to compare the diquark masses with corresponding bottomonium states, we can observe that except for 1^3S_1 state, the bb -diquark mass is significantly less than the corresponding bottomonium states. This is because of the fact that for 1^3S_1 state, the interaction is dominated by Coulomb interaction which is $-\frac{2\alpha_s}{3r}$ for bb -diquark and $-\frac{4\alpha_s}{3r}$ for bottomonium. This Coulomb interaction is greater for diquark resulting in higher interaction energy, thus resulting in higher mass. For excited states, the interaction is dominated by confinement part which is $\frac{\lambda(1-e^{-\nu r})}{2r}$ for bb -diquark and $\frac{\lambda(1-e^{-\nu r})}{r}$ for bottomonium. Here, the interaction energy will be lower for diquark resulting in lesser mass compared to corresponding bottomonium states.

III.3. Triply bottom baryons:

We have computed the mass spectra of triply bottom baryons using the diquark-quark model. The triply bottom baryons are modelled as a bound state of a bb -diquark and a b -quark. We have considered the radial and orbital excitations of both diquark and diquark-quark system. The computed mass spectra are presented in Tables VIII

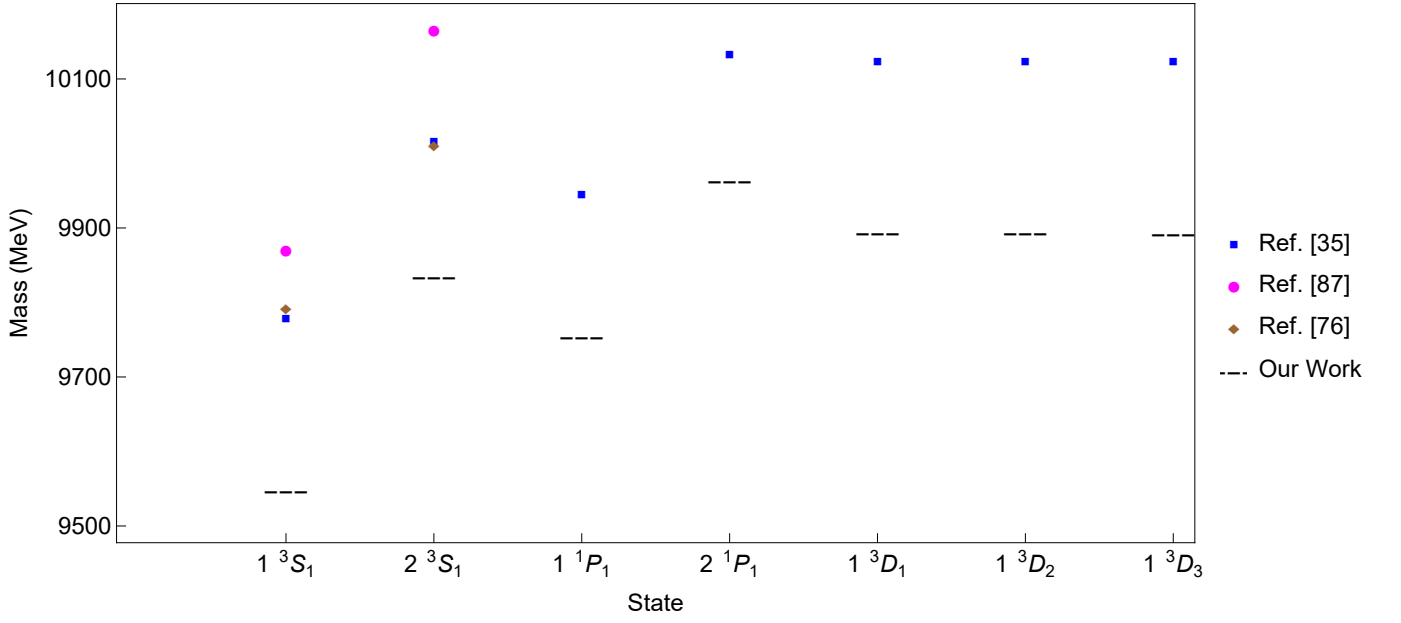


FIG. 3: Comparison of mass spectra of bb -diquark obtained from our model with other theoretical models in MeV.

TABLE VIII: Mass Spectra of bbb baryon in GeV (positive parity).

State	J^P	Mass	State	J^P	Mass	State	J^P	Mass	State	J^P	Mass
$1S1s$	$\frac{3}{2}^+$	14.243	$1S2s$	$\frac{3}{2}^+$	14.783	$2S1s$	$\frac{3}{2}^+$	14.528	$2S2s$	$\frac{3}{2}^+$	15.068
$1S1d$	$\frac{1}{2}^+$	14.917	$1S2d$	$\frac{1}{2}^+$	15.190	$2S1d$	$\frac{1}{2}^+$	15.202	$2S2d$	$\frac{1}{2}^+$	15.474
	$\frac{3}{2}^+$	14.922		$\frac{3}{2}^+$	15.194		$\frac{3}{2}^+$	15.207		$\frac{3}{2}^+$	15.478
	$\frac{5}{2}^+$	14.928		$\frac{5}{2}^+$	15.200		$\frac{5}{2}^+$	15.214		$\frac{5}{2}^+$	15.484
	$\frac{7}{2}^+$	14.936		$\frac{7}{2}^+$	15.206		$\frac{7}{2}^+$	15.221		$\frac{7}{2}^+$	15.490
$1P1p$	$\frac{1}{2}^+$	14.880	$1P2p$	$\frac{1}{2}^+$	15.216	$2P1p$	$\frac{1}{2}^+$	15.087	$2P2p$	$\frac{1}{2}^+$	15.428
	$\frac{3}{2}^+$	14.899		$\frac{3}{2}^+$	15.232		$\frac{3}{2}^+$	15.106		$\frac{3}{2}^+$	15.438
	$\frac{5}{2}^+$	14.915		$\frac{5}{2}^+$	15.244		$\frac{5}{2}^+$	15.122		$\frac{5}{2}^+$	15.450
$1D1s$	$\frac{3}{2}^+$	14.585	$1D2s$	$\frac{3}{2}^+$	15.125	$2D1s$	$\frac{3}{2}^+$	14.756	$2D2s$	$\frac{3}{2}^+$	15.295
$1D1d$	$\frac{1}{2}^+$	15.259	$1D2d$	$\frac{1}{2}^+$	15.532	$2D1d$	$\frac{1}{2}^+$	15.430	$2D2d$	$\frac{1}{2}^+$	15.702
	$\frac{3}{2}^+$	15.264		$\frac{3}{2}^+$	15.535		$\frac{3}{2}^+$	15.434		$\frac{3}{2}^+$	15.705
	$\frac{5}{2}^+$	15.271		$\frac{5}{2}^+$	15.541		$\frac{5}{2}^+$	15.441		$\frac{5}{2}^+$	15.711
	$\frac{7}{2}^+$	15.279		$\frac{7}{2}^+$	15.548		$\frac{7}{2}^+$	15.449		$\frac{7}{2}^+$	15.718

TABLE IX: Mass Spectra of bbb baryon in GeV (negative parity).

State	J^P	Mass	State	J^P	Mass	State	J^P	Mass	State	J^P	Mass
$1S1p$	$\frac{1}{2}^-$	14.694	$1S2p$	$\frac{1}{2}^-$	15.026	$2S1p$	$\frac{1}{2}^-$	14.979	$2S2p$	$\frac{1}{2}^-$	15.311
	$\frac{3}{2}^-$	14.700		$\frac{3}{2}^-$	15.031		$\frac{3}{2}^-$	14.985		$\frac{3}{2}^-$	15.316
$1P1s$	$\frac{1}{2}^-$	14.390	$1P2s$	$\frac{1}{2}^-$	14.967	$2P1s$	$\frac{1}{2}^-$	14.597	$2P2s$	$\frac{1}{2}^-$	15.174
$1P1d$	$\frac{3}{2}^-$	15.133	$1P2d$	$\frac{3}{2}^-$	15.403	$2P1d$	$\frac{3}{2}^-$	15.340	$2P2d$	$\frac{3}{2}^-$	15.610
	$\frac{5}{2}^-$	15.135		$\frac{5}{2}^-$	15.405		$\frac{5}{2}^-$	15.342		$\frac{5}{2}^-$	15.612
$1D1p$	$\frac{1}{2}^-$	15.037	$1D2p$	$\frac{1}{2}^-$	15.368	$2D1p$	$\frac{1}{2}^-$	15.207	$2D2p$	$\frac{1}{2}^-$	15.538
	$\frac{3}{2}^-$	15.043		$\frac{3}{2}^-$	15.373		$\frac{3}{2}^-$	15.213		$\frac{3}{2}^-$	15.543

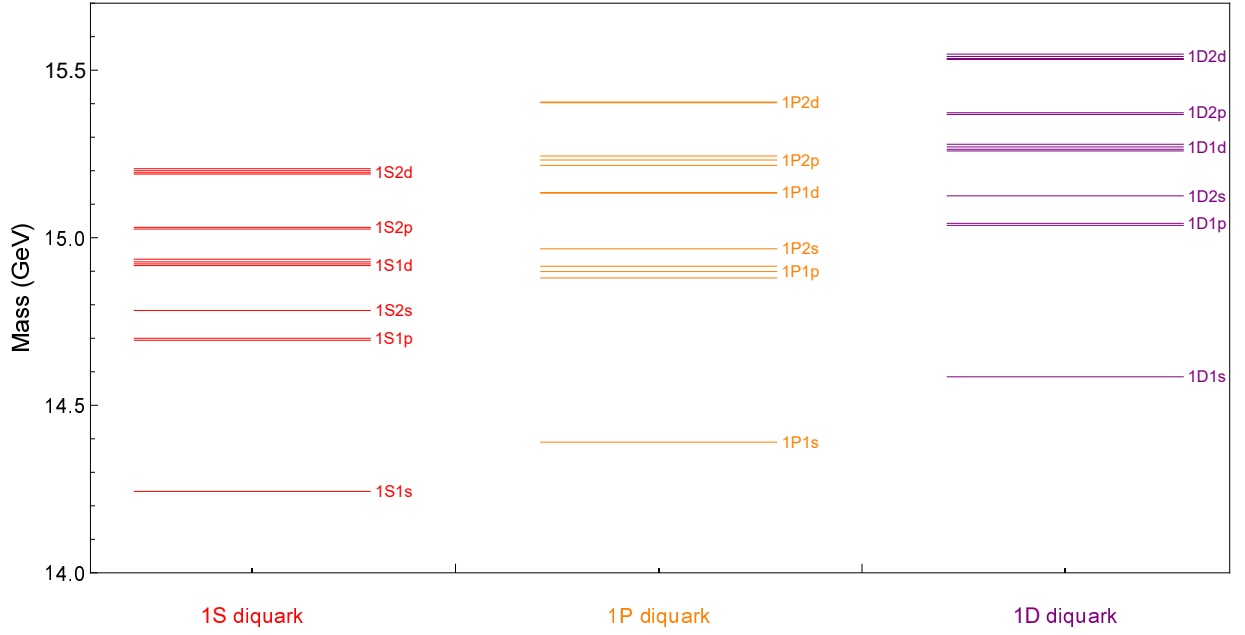


FIG. 4: Mass spectra of triply bottom baryons corresponding to different diquark states with $n_d = 1$.

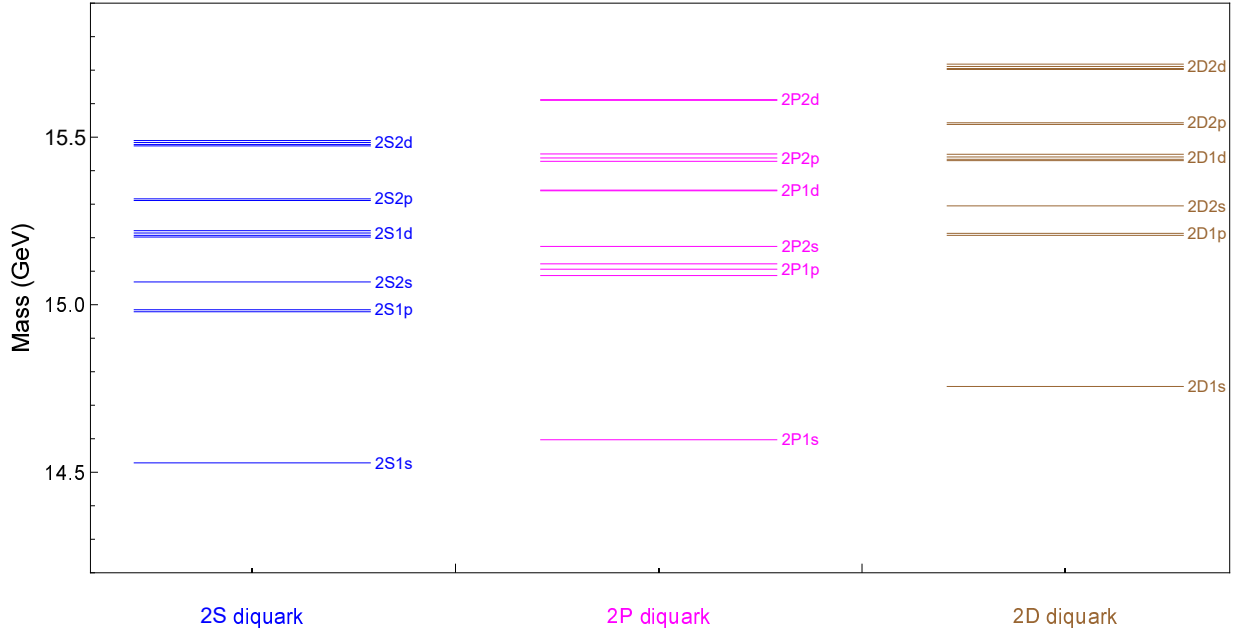


FIG. 5: Mass spectra of triply bottom baryons corresponding to different diquark states with $n_d = 2$.

corresponding to $J^P = \frac{5}{2}^+$ predicted from our model is 14.915 GeV (1P1p state) which is close to the mass predicted in Refs [17, 35, 41] but is less than around 378 MeV and 186 MeV from the mass predicted in Ref. [48] and [42] respectively. The lowest state mass corresponding to $J^P = \frac{7}{2}^+$ obtained from our model is 14.936 GeV (1S1d state) which is close to the mass obtained in Refs [17, 35, 41] but is less than around 350 MeV and 165 MeV from the mass obtained in Ref. [48] and [42] respectively. These differences in mass predictions may arise due to the differences in approaches employed and the differences in model parameters. Both in Refs [41] and [42], the masses of triply bottom baryons have been estimated within the constituent quark model with a linear confinement potential, but due to the differences in the parameters used, there are variations between the masses predicted from these models. The model parameters in Ref. [41] are obtained by fitting into the experimentally observed bottomonium states whereas in Ref. [42], the model parameters are obtained by fitting the experimentally observed singly bottom baryons. For $J^P = \frac{1}{2}^-$, the lowest state mass obtained from our model is 14.390 GeV (1P1s state) which is less than those predicted from

TABLE X: Comparison of ground state mass of triply bottom baryons with other theoretical approaches in GeV.

Approach	Mass
Constituent Quark Model [39]	14.396
Constituent Quark Model [41]	14.432
Constituent Quark Model [42]	14.834
Effective Quark Model [89]	15.129
Relativistic Quark Model [90]	14.569
Hypercentral Constituent Quark Model [48]	14.496
Faddev Equation [91]	14.370
Regge Phenomenology [92]	14.822
QCD Sum Rules [43]	13.28 ± 0.10
QCD Sum Rules [44]	14.3 ± 0.2
QCD Sum Rules [45]	14.43 ± 0.009
Diquark-quark Model [35]	14.468
Diquark-quark Model [93]	14.370
Our Work	14.243

TABLE XI: Comparison of masses of lowest state triply bottom baryons corresponding to different J^P values in GeV.

J^P	Our Work	[35]	[39]	[48]	[42]	[41]
$\frac{1}{2}^+$	14.880	14.877	14.894	15.306	15.097	14.959
$\frac{3}{2}^+$	14.243	14.468	14.396	14.496	14.834	14.432
$\frac{5}{2}^+$	14.915	14.895	14.894	15.293	15.101	14.981
$\frac{7}{2}^+$	14.936	14.909	14.894	15.286	15.101	14.988
$\frac{1}{2}^-$	14.390	14.698	14.688	14.944	14.975	14.773
$\frac{3}{2}^-$	14.700	14.702	14.688	14.937	14.976	14.779
$\frac{5}{2}^-$	15.135	15.081	15.038	14.931		

other models. For $J^P = \frac{3}{2}^-$, the lowest state mass obtained from our model is 14.700 GeV ($1S1p$ state) which is close to the mass obtained in Refs [17, 35, 41]. For $J^P = \frac{5}{2}^-$, the lowest mass obtained from our model is 15.135 GeV ($1P1d$ state) which is close to the mass predicted by Ref.s [17, 35, 41]. However, the validity of these theoretical models hinges on the experimental discovery of these states.

IV. SUMMARY:

In this work, we have evaluated the mass spectrum of bottomonium, $b\bar{b}$ -diquark, and triply bottom baryons by utilizing a phenomenological potential model comprising of short-range one-gluon Coulomb potential, a screened confinement potential, and $O(1/m)$ corrections predicted from pNRQCD and lattice studies. Unlike most models that use linear confinement potential, we have applied a screened confinement potential along with $O(1/m)$ correction terms to predict the mass spectra of beauty hadrons. This approach takes into account several features, including the flattening of the linear confinement potential as the separation between quarks increases, as well as the effects of finite heavy quark masses. The model parameters are obtained by fitting some of the experimentally well-established bottomonium states. The predicted masses of bottomonium are compared with other theoretical models and available experimental results. Below the $B\bar{B}$ threshold, the mass predicted from our model is close to the experimental values, whereas above this threshold, there are small deviations from the experimental results. The mass spectra of triply bottom baryons are evaluated within the diquark-quark model, and we have compared them with other theoretical models, as there are no experimental states discovered yet. Our predictions can help to narrow down the expected mass range for the experimental discovery of triply bottom baryons.

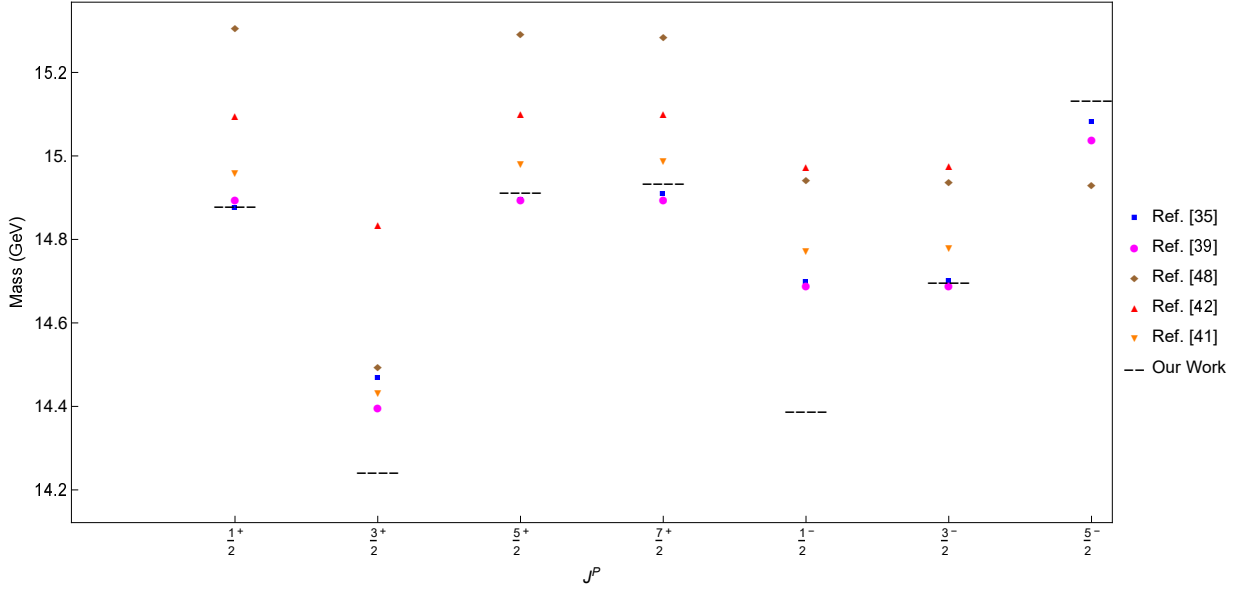


FIG. 6: Comparison of masses of lowest state triply bottom baryons corresponding to different J^P values in GeV.

ACKNOWLEDGMENTS

One of the authors (RK) is grateful to the Manipal Academy of Higher Education, Manipal for financial support under ‘Dr. TMA Pai Scholarship Programme’.

-
- [1] N. Brambilla, S. Eidelman, B. Heltsley, R. Vogt, G. Bodwin, E. Eichten, A. Frawley, A. Meyer, R. Mitchell, V. Papadimitriou, *et al.*, *Eur. Phys. J. C* **71**, 1 (2011).
 - [2] R. Mandal, B. Ananthanarayan, and D. Wyler, *Eur. Phys. J. Spec. Top.*, 1 (2024).
 - [3] N. Cabibbo, *Phys. Rev. Lett.* **10**, 531 (1963).
 - [4] M. Kobayashi and T. Maskawa, *Prog. Theor. Phys.* **49**, 652 (1973).
 - [5] S. Herb, D. Hom, L. Lederman, J. Sens, H. Snyder, J. Yoh, J. Appel, B. Brown, C. Brown, W. Innes, *et al.*, *Phys. Rev. Lett.* **39**, 252 (1977).
 - [6] W. R. Innes, J. Appel, B. Brown, C. Brown, K. Ueno, T. Yamanouchi, S. Herb, D. Hom, L. Lederman, J. Sens, *et al.*, *Phys. Rev. Lett.* **39**, 1240 (1977).
 - [7] T. Skwarnicki, D. Antreasyan, D. Besset, J. Bienlein, E. Bloom, I. Brock, R. Cabenda, A. Cartacci, M. Cavalli-Sforza, R. Clare, *et al.*, *Phys. Rev. Lett.* **58**, 972 (1987).
 - [8] G. Bonvicini, D. Cinabro, M. Dubrovin, A. Bornheim, E. Lipeles, S. Pappas, A. Shapiro, A. Weinstein, R. A. Briere, G. Chen, *et al.*, *Phys. Rev. D* **70**, 032001 (2004).
 - [9] S. Dobbs, Z. Metreveli, A. Tomaradze, T. Xiao, and K. K. Seth, *Phys. Rev. Lett* **109**, 082001 (2012).
 - [10] S. Dobbs and C. Collaboration, in *AIP Conference Proceedings*, Vol. 1257 (American Institute of Physics, 2010) pp. 408–412.
 - [11] M. Artuso, C. Boulahouache, S. Blusk, J. Butt, E. Dambasuren, O. Dorjkhaidav, J. Li, N. Menaa, R. Mountain, H. Muramatsu, *et al.*, *Phys. Rev. Lett* **94**, 032001 (2005).
 - [12] R. Mizuk, D. Asner, A. Bondar, T. Pedlar, I. Adachi, H. Aihara, K. Arinstein, V. Aulchenko, T. Aushev, T. Aziz, *et al.*, *Phys. Rev. Lett* **109**, 232002 (2012).
 - [13] A. Bondar, A. Garmash, R. Mizuk, D. Santel, K. Kinoshita, I. Adachi, H. Aihara, K. Arinstein, D. Asner, T. Aushev, *et al.*, *Phys. Rev. Lett* **108**, 122001 (2012).
 - [14] R. Mizuk, A. Bondar, I. Adachi, H. Aihara, D. Asner, V. Aulchenko, T. Aushev, R. Ayad, I. Badhrees, S. Bahinipati, *et al.*, *J. High Energy Phys.* **2019** (10), 1.
 - [15] B. Aubert, M. Bona, Y. Karyotakis, J. Lees, V. Poireau, E. Prencipe, X. Prudent, V. Tisserand, J. Garra Tico, E. Grauges, *et al.*, *Phys. Rev. Lett* **102**, 012001 (2009).
 - [16] B. Aubert, R. Barate, D. Boutigny, F. Couderc, J.-M. Gaillard, A. Hicheur, Y. Karyotakis, J. Lees, V. Tisserand, A. Zghiche, *et al.*, *Phys. Rev. D* **72**, 032005 (2005).
 - [17] J. Lees, V. Poireau, V. Tisserand, E. Grauges, A. Palano, G. Eigen, B. Stugu, D. N. Brown, L. Kerth, Y. G. Kolomensky, *et al.*, *Phys. Rev. D* **90**, 112010 (2014).

- [18] J. Lees, V. Poireau, V. Tisserand, J. Garra Tico, E. Grauges, M. Martinelli, D. Milanese, A. Palano, M. Pappagallo, G. Eigen, *et al.*, Phys. Rev. D **84**, 011104 (2011).
- [19] G. Aad, B. Abbott, J. Abdallah, A. A. Abdelalim, A. Abdesselam, O. Abidinov, B. Abi, M. Abolins, O. Abouzeid, H. Abramowicz, *et al.*, Phys. Rev. Lett **108**, 152001 (2012).
- [20] A. M. Sirunyan, A. Tumasyan, W. Adam, F. Ambrogio, E. Asilar, T. Bergauer, J. Brandstetter, M. Dragicevic, J. Erö, A. Escalante Del Valle, *et al.*, Phys. Rev. Lett **121**, 092002 (2018).
- [21] R. Aaij, B. Adeva, M. Adinolfi, A. Affolder, Z. Ajaltouni, S. Akar, J. Albrecht, F. Alessio, M. Alexander, S. Ali, *et al.*, J. High Energy Phys. **2014** (10), 1.
- [22] T. Aaltonen, A. Abulencia, J. Adelman, T. Affolder, T. Akimoto, M. G. Albrow, S. Amerio, D. Amidei, A. Anastassov, K. Anikeev, *et al.*, Phys. Rev. Lett. **99**, 202001 (2007).
- [23] S. Navas, C. Amsler, T. Gutsche, C. Hanhart, J. Hernández-Rey, C. Lourenço, A. Masoni, M. Mikhasenko, R. Mitchell, C. Patrignani, *et al.*, Phys. Rev. D **110**, 030001 (2024).
- [24] M. G. Nobary, Phys. Lett. B **559**, 239 (2003).
- [25] Y.-Q. Chen and S.-Z. Wu, J. High Energy Phys. **2011** (8), 1.
- [26] M. Neubert, Proceedings, Summer School in Particle Physics , 244 (2000).
- [27] A. collaboration, arXiv preprint arXiv:2211.02491 10.48550/arXiv.2211.02491 (2022).
- [28] Y. Koma and M. Koma, Few-Body Syst. **54**, 1027 (2013).
- [29] N. Brambilla, A. Pineda, J. Soto, and A. Vairo, Rev. Mod. Phys. **77**, 1423 (2005).
- [30] N. Brambilla, M. A. Escobedo, J. Soto, and A. Vairo, Phys. Rev. D **97**, 074009 (2018).
- [31] Y. Yan, Y. Wu, and W. Wang, Int. J. Mod. Phys. A **15**, 2735 (2000).
- [32] S. Meinel, Phys. Rev. D **79**, 094501 (2009).
- [33] T. Onogi, Int. J. Mod. Phys. A **24**, 4607 (2009).
- [34] S. Meinel, Phys. Rev. D **85**, 114510 (2012).
- [35] R. Faustov and V. Galkin, Phys. Rev. D **105**, 014013 (2022).
- [36] D. Ebert, R. Faustov, V. Galkin, and A. Martynenko, Phys. Rev. D **66**, 014008 (2002).
- [37] R. Chaturvedi, A. K. Rai, N. R. Soni, and J. N. Pandya, J. Phys. G **47**, 115003 (2020).
- [38] L. Bai-Qing and C. Kuang-Ta, Commun. Theor. Phys. **52**, 653 (2009).
- [39] G. Yang, J. Ping, P. G. Ortega, and J. Segovia, Chin. Phys. C **44**, 023102 (2020).
- [40] J. Vijande, A. Valcarce, and H. Garcilazo, Phys. Rev. D **91**, 054011 (2015).
- [41] M.-S. Liu, Q.-F. Lü, and X.-H. Zhong, Phys. Rev. D **101**, 074031 (2020).
- [42] W. Roberts and M. Pervin, Int. J. Mod. Phys. A **23**, 2817 (2008).
- [43] J.-R. Zhang and M.-Q. Huang, Phys. Lett. B **674**, 28 (2009).
- [44] T. M. Aliev, K. Azizi, and M. Savci, J. Phys. G **41**, 065003 (2014).
- [45] Z.-G. Wang, AAPPs Bulletin **31**, 5 (2021).
- [46] P.-L. Yin, C. Chen, G. Krein, C. D. Roberts, J. Segovia, and S.-S. Xu, Phys. Rev. D **100**, 034008 (2019).
- [47] Z. S. Brown, W. Detmold, S. Meinel, and K. Orginos, Phys. Rev. D **90**, 094507 (2014).
- [48] Z. Shah and A. K. Rai, Eur. Phys. J. A **53**, 1 (2017).
- [49] B. Patel, A. Majethiya, and P. Vinodkumar, Pramana **72**, 679 (2009).
- [50] E. Klempt and J.-M. Richard, Rev. Mod. Phys. **82**, 1095 (2010).
- [51] S. Capstick and W. Roberts, Prog. Part. Nucl. Phys. **45**, S241 (2000).
- [52] M. Y. Barabanov, M. Bedolla, W. Brooks, G. Cates, C. Chen, Y. Chen, E. Cisbani, M. Ding, G. Eichmann, R. Ent, *et al.*, Prog. Part. Nucl. Phys. **116**, 103835 (2021).
- [53] M. Gell-Mann, Phys. Lett **8**, 214 (1964).
- [54] M. Anselmino, E. Predazzi, S. Ekelin, S. Fredriksson, and D. Lichtenberg, Rev. Mod. Phys. **65**, 1199 (1993).
- [55] H. Mutuk, Eur. Phys. J. Plus **137**, 1 (2022).
- [56] G. S. Bali, Phys. Rep. **343**, 1 (2001).
- [57] G. S. Bali, C. Schlichter, and K. Schilling, Phys. Rev. D **51**, 5165 (1995).
- [58] M. Sreelakshmi and A. Ranjan, J. Phys. G **50**, 073001 (2023).
- [59] Y.-B. Ding, K.-T. Chao, and D.-H. Qin, Phys. Rev. D **51**, 5064 (1995).
- [60] Y. Koma, M. Koma, and H. Wittig, Phys. Rev. Lett **97**, 122003 (2006).
- [61] A. Bhaghyesh, Adv. High Energy Phys. **2021**, 1 (2021).
- [62] S. M. Ikhdair, Eur. Phys. J. A **39**, 307 (2009).
- [63] W. Lucha and F. F. Schöberl, Int. J. Mod. Phys. C **10**, 607 (1999).
- [64] M. Pillai, J. Goglio, and T. G. Walker, Am. J. Phys. **80**, 1017 (2012).
- [65] F. Brau and C. Semay, J. Comput. Phys. **139**, 127 (1998).
- [66] A. Vega and J. Flores, Pramana **87**, 1 (2016).
- [67] G. Esposito and P. Santorelli, Eur. Phys. J. Plus **137**, 642 (2022).
- [68] H. Mutuk, Can. J. Phys. **97**, 1342 (2019).
- [69] T. Nayana and A. Bhaghyesh, Int. J. Mod. Phys. A **39**, 2450101 (2024).
- [70] V. R. Debastiani and F. S. Navarra, Chin. Phys. C **43**, 013105 (2019).
- [71] T. Barnes, S. Godfrey, and E. Swanson, Phys. Rev. D **72**, 054026 (2005).
- [72] N. Soni, B. Joshi, R. Shah, H. Chauhan, and J. Pandya, Eur. Phys. J. C **78**, 1 (2018).
- [73] J.-Z. Wang, Z.-F. Sun, X. Liu, and T. Matsuki, Eur. Phys. J. C **78**, 1 (2018).
- [74] W. Lucha, F. F. Schöberl, and D. Gromes, Physics reports **200**, 127 (1991).
- [75] D. Griffiths, *Introduction to elementary particles* (John Wiley & Sons, 2020).

- [76] H. Mutuk, Eur. Phys. J. C **81**, 367 (2021).
- [77] E. Eichten and F. Feinberg, Phys. Rev. D **23**, 2724 (1981).
- [78] D. Gromes, Z. Phys. C **26**, 401 (1984).
- [79] P. Jakhad, J. Oudichhya, K. Gandhi, and A. K. Rai, Phys. Rev. D **108**, 014011 (2023).
- [80] V. Kher, R. Chaturvedi, N. Devlani, and A. Rai, Eur. Phys. J. Plus **137**, 357 (2022).
- [81] B. Pandya, M. Shah, and P. Vinodkumar, Eur. Phys. J. C **81**, 1 (2021).
- [82] I. Asghar and N. Akbar, Eur. Phys. J. A **60**, 58 (2024).
- [83] A. Badalian, B. Bakker, and I. Danilkin, Phys. Rev. D **79**, 037505 (2009).
- [84] Z. Zhao, K. Xu, A. Limphirat, W. Sreethawong, N. Tagsinsit, A. Kaewsnod, X. Liu, K. Khosonthongkee, S. Cheedket, and Y. Yan, Phys. Rev. D **109**, 016012 (2024).
- [85] C. A. Bokade and B. Azhothkaran, Chin. Phys. C 10.1088/1674-1137/adc084 (2025).
- [86] Y. A. Simonov and A. Veselov, Phys. Rev. D **79**, 034024 (2009).
- [87] F. Giannuzzi, Phys. Rev. D **79**, 094002 (2009).
- [88] B. Eakins and W. Roberts, Int. J. Mod. Phys. A **27**, 1250039 (2012).
- [89] R. Dhir, C. Kim, and R. Verma, Phys. Rev. D **88**, 094002 (2013).
- [90] A. Martynenko, Phys. Lett. B **663**, 317 (2008).
- [91] S.-X. Qin, C. D. Roberts, and S. M. Schmidt, Few-Body Syst. **60**, 1 (2019).
- [92] J. Oudichhya, K. Gandhi, and A. K. Rai, Phys. Rev. D **104**, 114027 (2021).
- [93] K. Thakkar, A. Majethiya, and P. Vinodkumar, Eur. Phys. J. Plus **131**, 339 (2016).